韓國海洋工學會誌 第12卷 第1號, pp.143~152, 1998. 2

◉ 論 文

Liquefaction in Seabeds and Stability of Coastal Structure Foundations

Hong-Yoon Kang* · Ik-Hyo Lee**

(97년 10월 20일 접수)

해저지반의 액상화와 해안구조물 기초의 안정성

강 홍 윤* · 이 익 효**

Key Words : Foundation (기초), Seabed (해저지반), Wave (파랑), Liquefaction (액상화), Coastal Structures (해안구조물), Soil (토질)

초 록

해안구조물 설치시 기초지반의 안정성 해석을 위해 파랑에 기인한 액상화 메카니즘을 과잉간극수압 (excess pore pressure) 현상과 관련하여 논의하였다. 과잉간극수압 발생 메커니즘에 있어서 두 가지 형태, 즉, 변동과잉간극수압 (Oscillatory excess pore pressure) 및 잔류과잉간극수압 (Residual excess pore pressure) 각각에 기인한 액상화의 특성을 구명하였다. 또한, 과잉간극수압 및 해저지반의 액상화 가능성에 대한 평가공정을 제시하였는데 이는 모형실험과 현장관측자료에 의해 그 적용성이 검증되었다. 이러한 평가공정 (Assessment Procedures)은 투수성 해저/기초 지반의 액상화를 추정하는데 이용될 수 있다. 해안구조물 기초 설계 및 해저지반의 안정성 평가시 액상화의 가능성 또는 과잉간극수압의 적절한 평가·고려가 무엇보다 중요하다고 사료된다.

1. INTRODUCTION

Propagating ocean waves create dynamic water pressures on a seabed surface or a beach face[1]. In response to these wave-associated bottom pressures, excess pore pressures are produced in the seabed. When the excess pore pressures become large enough, the liquefaction of permeable seabed may occur, causing some damages of offshore and coastal structures[2].

There are two types of wave-induced excess pore pressures treated in the previous works: one is the 'oscillatory' or 'transient' nature of excess pore pressures and the other is the

* 정회원, Post Doctoral Fellow, Center for Applied Coastal Research, University of Delaware, Newark, Delaware 19716, U.S.A.

**정회원, 여수대학교 해양토목공학과 교수

'residual' or 'progressive' nature of excess pore pressures. The former is resulted from damping and phase lags of the pore pressures at the seabed in the propagation process of the wave-associated bottom pressures[3]. Whereas, the latter is induced by the cyclic shear stresses which are generated by the differential loading of the seabed from the bottom pressures varying harmonically in time and space[4]. They are also induced by the cyclic shear stresses transferred through the interface between the structure and the seabed[5].

In view of the literature on wave-driven liquefaction and foundation/seabed stability, few experimental studies have been reported.

This paper thus clarifies both the above mentioned types of wave-driven liquefaction experimentally and presents the procedures for assessing the liquefaction potential. The applicability of the procedures in practical problems is also examined.

2. WAVE-DRIVEN LIQUEFACTION TYPES

The excess pore pressure is one of the comprehensive parameters in evaluating the liquefaction potential. The excess pore pressures may lead to the liquefaction of seabed sands at a moment when they attain the identical values of the initial vertical effective stresses at calm sea.

Wave-driven liquefaction is classified into two categories in terms of the mechanism of the excess pore pressure build-up. Different responses of the excess pore pressures are schematically illustrated in Fig. 1.

The liquefaction due to the oscillatory nature of excess pore pressures (hereafter referred to as the oscillatory excess pore pressure) occurs transiently and appears periodically so many times during storm waves, responding to each wave. The liquefaction due to the residual nature of excess pore pressures (hereafter referred to as the residual excess pore pressure) depends on intensity and duration of wave loading, and more dominantly on the dissipation of generated pore pressures. This type of liquefaction is similar to that induced by earthquakes in the mechanism of the excess pore pressure build-up. The liquefaction occurs at once after certain numbers of cyclic wave loading.

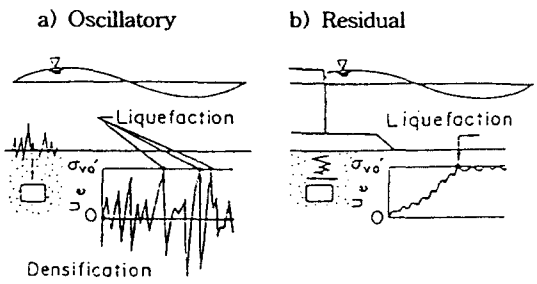

Fig. 1 Different Responses of Excess pore pressures

The total excess pore pressures to cause the liquefaction should be the superposition of both the oscillatory and residual excess pore pressures. Which type of excess pore pressure is more dominant to the liquefaction is considered to depend on the wave characteristics, soil and pore water properties and configuration of seabed.

3. PROCEDURES FOR ASSESSING LIQUEFACTION POTENTIAL

3.1 Excess Pore Pressure

Two types of wave-driven excess pore pressures are incorporated into a consolidation equation under two dimensional plain strain conditions:

$$C_v \nabla^2 u_e = \alpha \frac{\partial u_e}{\partial t} + (\alpha - 1) \frac{\partial p_b}{\partial t} - \frac{\partial u_g}{\partial t} \qquad (1)$$

where ue is the excess pore pressure (the total of the oscillatory and residual components), p_b

the wave-associated water pressure at the seabed surface, u_g the excess pore pressure generated by the cyclic shear stress under undrained conditions, C_v the coefficient of consolidation and α the coefficient of propagation. the α is given by

$$\alpha = 1+\frac{nm_w}{m_v} \tag{2}$$

where n = the porosity, m_v = the coefficient of volume compressibility and m_w = the compressibility of pore water. The $\partial u_g/\partial t$ means the generation rate of excess pore pressures due to the cyclic shear stress under undrained conditions. When α is equal to 1, Eq. (1) becomes the same equation as that presented by Rahman et al.[6]. If the $\partial u_g/\partial t$ is so small as to be ignored, Eq.(1) becomes identical with the consolidation equation.

3.2 Liquefaction Criterion

The shear strength of seabed, τ_f, is given by

$$\tau_f = (\sigma'_{no} - u_e) \cdot \tan\phi' \tag{3}$$

where σ'_{no} = the normal effective stress at calm sea and ϕ' = the internal friction angle. The normal effective stress during storm waves vary in response to the wave-induced excess pore pressure, u_e. If u_e becomes larger than σ'_{no}, seabed sands liquefy and lose the shear strength. The liquefaction criterion can be expressed as :

$$\sigma'_{no} \leq u_e \tag{4}$$

4. EXCESS PORE PRESSURE AND LIQUEFACTION

4.1 Oscillatory Excess Pore Pressure and Liquefaction

When the wave length is large enough compared with the thickness of permeable seabed, we may consider the liquefaction phenomenon under one dimensional plain strain condition of seabed. Provided that the residual excess pore pressures are so small as to be ignored, the excess pore pressures are represented by the oscillatory excess pore pressures given by Eq. (5)[3),7)] :

$$u_e = -(p_b - p_m) \tag{5}$$

The vertical effective stress, σ'_v, is thus expressed as

$$\sigma'_v = \sigma'_{vo} + (p_b - p_m) \tag{6}$$

where p_b = wave-associated water pressure at the seabed surface, p_m = oscillatory pore pressure in the seabed and σ'_{vo} = initial vertical effective stress in the seabed at calm sea. Substituting Eq. (5) into Eq. (1) and omitting $\partial u_g/\partial t$ gives

$$C_v\frac{\partial^2 p_m}{\partial z^2} = \alpha\frac{\partial p_m}{\partial t} - \frac{\partial p_b}{\partial t} \tag{7}$$

The liquefaction criterion is written by setting the σ'_v in Eq. (6) equal to or less than zero:

$$\sigma'_{vo} \leq u_e = -(p_b - p_m) \tag{8}$$

The p_m is calculated using Eq. (7) under appropriate boundary and initial conditions. The p_b is approximately determined by the linear wave theory. The σ'_{vo} is calculated with the submerged unit weight of deposits. If we introduce the p_b, p_m and σ'_{vo} into Eq. (8), we can assess the liquefaction potential.

In order to examine the applicability of Eqs. (5) through (8), laboratory data[3),7)] and field data[8)] were used. Fig. 2 shows comparisons between calculated and measured oscillatory pore pressures in the seabed. The finite difference method was employed to solve Eq. (7) under one

dimensional condition. The calculated trains of oscillatory pore pressures and effective vertical stress ratios are fairly well consistent with the measured ones.

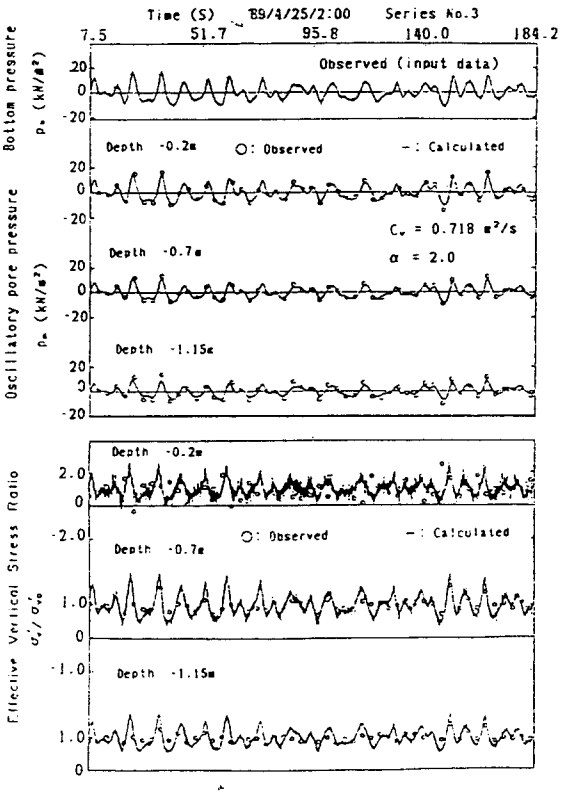

Fig. 2 Comparisons of observed and calculated oscillatory pore pressures and stress ratios in the seabed

It is found from Fig. 2 that the stress ratio at the depth of 0.2 m repeatedly attains zero or less under wave trough. This suggests that the liquefaction may occur at that depth.

In Fig. 3, the wave-induced vertical effective stresses are compared with the initial vertical effective stresses at calm sea. According to the liquefaction criterion given by Eq. (8), the liquefied depth is observed at the depth shallower than 0.2 m.

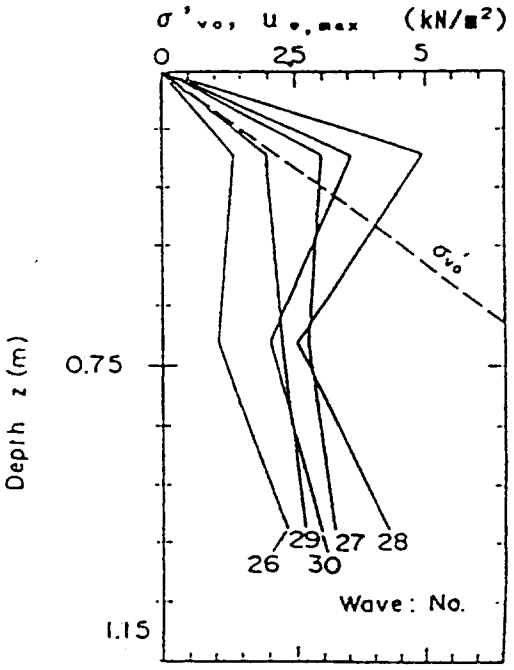

Fig. 3 Liquefaction at calm sea (field data)

4.2 Seepage Force and Quick Sand

Seeing the liquefaction from different points of view, the seepage force may be considered another reason for the wave-driven liquefaction. As the increment of the vertical effective stress is given by

$$\frac{\partial \sigma'_v}{\partial z} = j + r' \tag{9}$$

Integration of Eq. (9) yields the vertical effective stress given by

$$\sigma'_v = \int_o^z j\,dz + r'z \tag{10}$$

The seepage force, j, is derived from Eqs. (6) and (9) by taking $\partial \sigma'_{vo}/\partial z = r'$ and $\partial p_b/\partial z = 0$ into account :

$$j = -\frac{\partial p_m}{\partial t} \tag{11}$$

The hydraulic gradient, i, and velocity, v, respectively, are given by

$$i = \frac{j}{r_w} \tag{12}$$

$$v = ki \tag{13}$$

where r' is the submerged unit weight of deposits, r_w the unit weight of pore water and k the coefficient of permeability.

Fig. 4 shows the distributions of j, i, v and the vertical effective stresses in the seabed. The open circles in Fig. 4 are calculated results from Eq. (10). The liquefied zone is found at depths shallower than 0.15 m. The vertical effective stresses can be computed by another procedure using Eq. (6). The results of the calculation are shown by the solid curve in Fig. 4. The liquefied zones in both calculations are consistent quite well each other.

The hydraulic gradient and seepage force in the liquefied zone become considerably large, resulting a kind of quick sand in the shallow depths where the overburden pressures are very small. It may be concluded that the wave-driven liquefaction is attributed to such a upward seepage flow in the seabed.

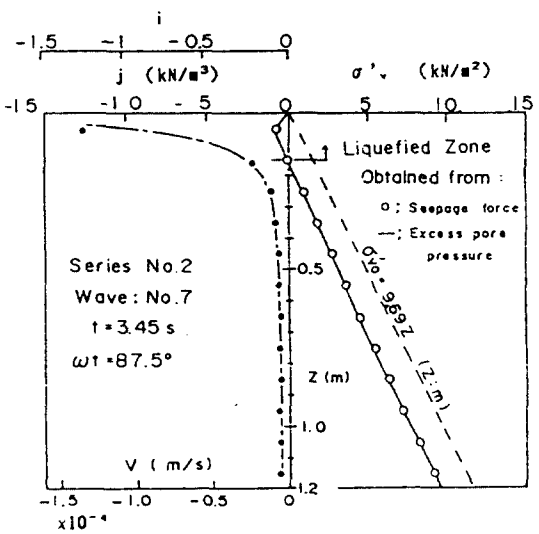

Fig. 4 Seepage forces and vertical effective stresses

4.3 Residual Excess Pore Pressure and Liquefaction

Measurements of the residual pore pressures in the model seabed have been reported by Zen et al.[9),10)]. Their laboratory data were adopted to compare with calculated results from this study.

Fig. 5 shows test cases where three types of seabed models were constituted. The clay layers were constructed by consolidating a slurry of clay in a model tank. The sand layer and sand seams were placed on the clay layer after the completion of consolidation. The relative density of sand is 40% to 50%. The permeability of sand deposits was decreased to $(1/30)^{0.5}$ using a polymer liquid, referred to as FLOC in Fig. 5, instead of water except for test case No.1. The value of $(1/30)^{0.5}$ was determined by taking account of the model scale of 1/30 and wave period on the basis of the Froude model law. The sinusoidal wave forms of horizontal loading with the periods of 13.5s and 2.5s were mechanically applied to a model caisson. The oscillatory excess pore pressures, thus, were not induced for sand deposits.

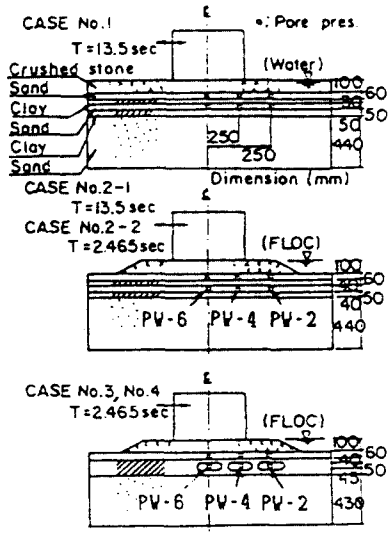

Fig. 5 Test cases

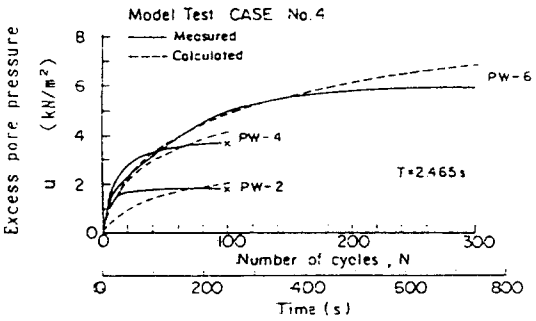

Fig. 6 Measured and calculated pore pressures

Measured and calculated residual excess pore pressures at the points denoted by PW-2, PW-4 and PW-6 in Fig. 5 are depicted in Fig. 6. Finite element method was employed to solve Eq. (1) under two dimensional plain strain conditions. The generation rate of excess pore pressures, $\partial u_g / \partial t$, is experimentally determined from the cyclic triaxial test. It is seen in Fig. 6 that the calculated residual excess pore pressures coincide with the measured ones. Eq. (1) can be used to estimate the residual excess pore pressures.

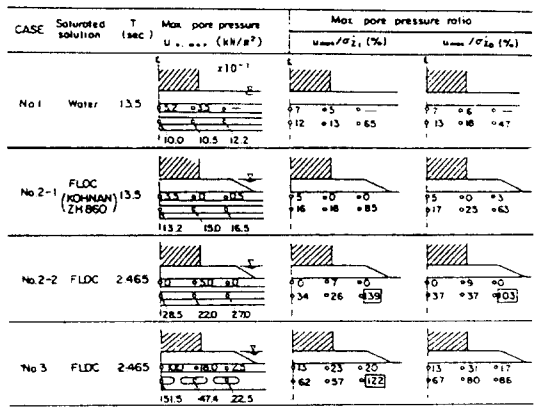

Fig. 7 Pore pressure ratio (σ'_{z1}: Boussinesq solution, σ'_{z0}: Boston code)

The stress ratios in the model seabed are illustrated in Fig. 7. In test cases No. 1 and No. 2-1, the stress ratios indicate less than 1.0 at all measuring points. Whereas, in test cases of Nos. 2-2 and 3, the stress ratios are definitely beyond 1.0 in sand deposits beneath the edge of the rubble mound. This means that the excess pore pressures to cause the liquefaction are locally stored in sand deposits. When the generated excess pore pressures are restricted to dissipate, seabed deposits are considered susceptible to liquefaction.

5. APPLICATION TO PRACTICAL PROBLEMS

5.1 Scouring and Instability of Detached Breakwater

The extensive local scour at the edge of a detached breakwater foundation has been observed. A large number of concrete blocks, which composed the detached breakwater at coast, have been found widely and deeply spread in the seabed. These phenomena are supposed closely related to the wave-driven liquefaction of seabed sands because once the liquefaction occurs in the seabed, the seabed loses the shear strength and the suspended sand particles are very easily transported by currents.

The liquefaction potential was evaluated by use of the procedures presented in the previous section, and was introduced into the stability analysis of the foundation. The p_b is estimated from the wave characteristics observed near the site using the linear wave theory. The p_m is calculated from Eq. (7). The liquefaction depth is assessed using Eq. (8). The input data for the analysis are the wave height H_{max} = 7.2 m, the wave period T = 11.8s, the coefficient of propagation α = 2.0, the coefficient of consolidation C_v = 0.71 m^2/s, the submerged unit weight of deposits is 9 kN/m^3 and the thickness of permeable seabed is 20.5m. The liquefaction depth at the edge of the rubble mound attains 1.25m in maximum under wave trough as

depicted in Fig. 8.

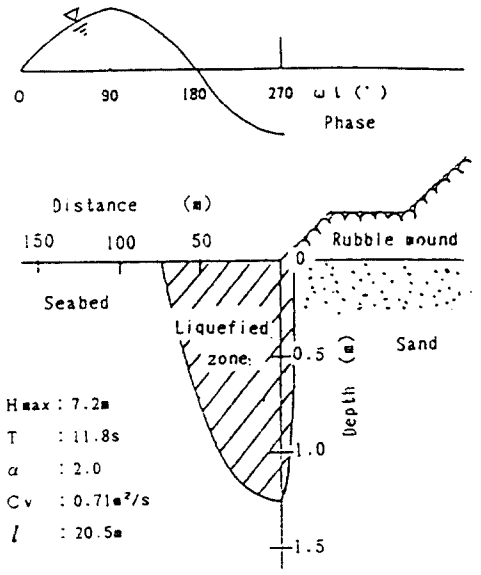

Fig. 8 Liquefied zone

The stability of coastal structures will decrease when the seabed is liquefied by waves. Fig. 9 shows the circular failure of the sloping breakwater after the liquefaction. The safety factor at calm sea was more than 1.3, but it decreases to 0.9 due to the liquefaction in seabed sands. The submergence of concrete blocks into the seabed reported so far can be attributed to such a liquefaction-related instability of seabed.

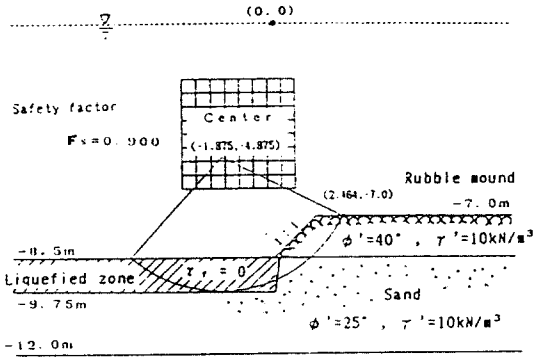

Fig. 9 Circular failure

The liquefied zone in Fig. 8 is computed for one wave only. Provided that the liquefied sand particles are completely transported after the liquefaction and no sand particles are supplied there, the scoured area gradually spreads widely and deeply in the seabed until no liquefaction occurs in the seabed. Thus, the wave-driven liquefaction is considered one of the significant reasons related to the scouring of seabeds. The accuracy of the estimation of scouring zone will be improved if the flow mechanism of liquefied sand particles is properly evaluated.

5.2 Residual Excess Pore Pressure and Circular Failure of Coastal structures

It has been reported that a breakwater in an exposed environment of the west port of Niigata, Japan, was critically damaged when an extra-tropical cyclone passed through the Japan sea on 29th of Oct. 1976. The largest dislocation of the caisson was the landward sliding by 4.5 m and the seaward tilt by 20 degrees. The mode of failure suggested a circular failure of the coastal structure foundation. The coastal structure (breakwater) was originally designed so as to be safe against circular slip failures according to the current design code, but the cyclic effects of wave loading were not taken into account.

The wave data recorded at the observation point near the breakwater have shown that the maximum wave height was 10 m and the maximum wave period was 13.5s. These wave characteristics correspond well to those of 50-years storm waves estimated in the design procedure. The design wave height of 7.0 m in terms of the significant wave height was determined in front of the breakwater, taking account of transformation of waves. A detailed soil investigation after the storm revealed that the soil profile was very complicated, being

composed of the thin sand layers and silty layers with sand seams. The undisturbed sands were sampled from the seabed and used for the triaxial cyclic tests and other laboratory tests to examine the possibility of the wave-driven liquefaction.

The generation rate of excess pore pressures, $\partial u_g/\partial t$, is formulated as Eq. (14) to introduce into Eq. (1)[10] :

$$\frac{\partial u_g}{\partial t} = \frac{\sigma'_{mo}(A/B)\,2\gamma B\exp(\lambda\gamma)}{2\gamma NB\exp(\lambda\gamma)}\frac{\partial N}{\partial t} \qquad (14)$$

where σ'_{mo} denotes the mean principal stress, A, B and λ the experimental constants, N the number of cycles, and γ the shear strain amplitude. The constants A, B and λ were, respectively, determined from the cyclic tests as 33.8, 258.6 and 549.0. Eq. (14) was employed to solve Eq. (1) with the same procedures as previously mentioned. The finite element method was used to calculate the shear strain amplitude, γ, caused by the wave loading through the interface between the caisson and foundation.

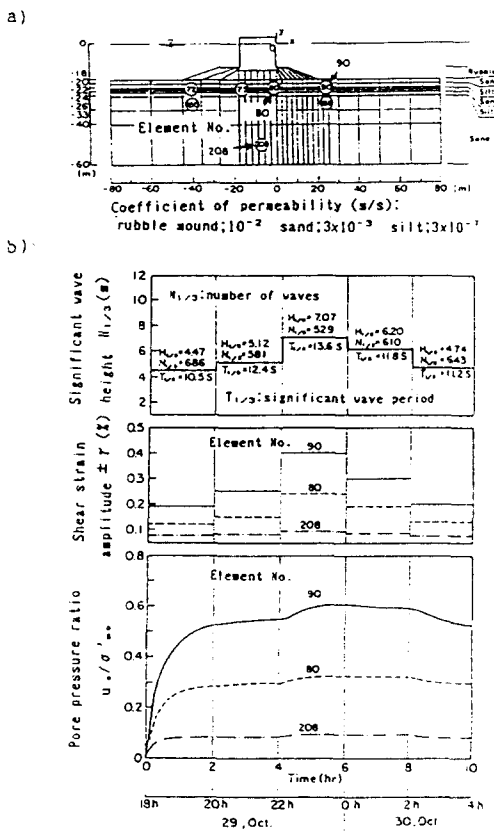

Fig. 10 Time history of pore pressure: a) Finite element model, b) Pore pressure ratio

The computed time histories of the residual excess pore pressures in terms of the pressure ratio are illustrated in Fig. 10. Observed wave characteristics are represented by the significant wave heights and periods every two hours. It is found in Fig. 10 that the pore pressure ratios increase up to 0.6 in the sand layer at the edge of the rubble mound, say at the element No. 90.

The comparisons between the calculated slip lines and the trace of the movement of caissons are shown in Fig. 11. Though the latter is not exactly the trace of the one caisson, it can be thought to represent the continuous movement of a caisson. The solid slip lines indicate the calculations in which the strength reductions due to excess pore pressure build-up are taken into account (referred to the cyclic wave loading in Fig. 11). The dotted ones show that the reductions are not considered (referred to the static wave loading in Fig. 11). The safety factors in the cyclic loading yield smaller values than those in the static loading. It is interesting to note that the slip line giving the safety factor 0.98 coincides with the trace of caissons.

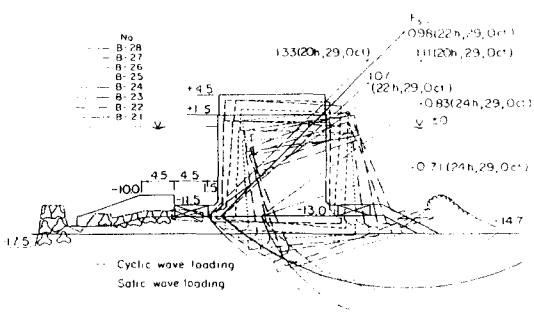

Fig. 11 Slip lines

The safety factors against the circular failure for three level of wave heights are presented in Fig. 12. The safety factor decreases by about 0.1 when the residual excess pore pressures are considered in the analysis. In other words, the critical wave height computed in consideration of cyclic loading effect is lessened by 1.5 m from that obtained from the static analysis. the conventional static analysis leads to dangerous evaluation of the safety factor in such a case that the generated excess pore pressures are restricted to dissipate by the existence of low permeability layers. Therefore, the wave-driven residual excess pore pressures should appropriately be taken into account for the design of coastal structure foundations.

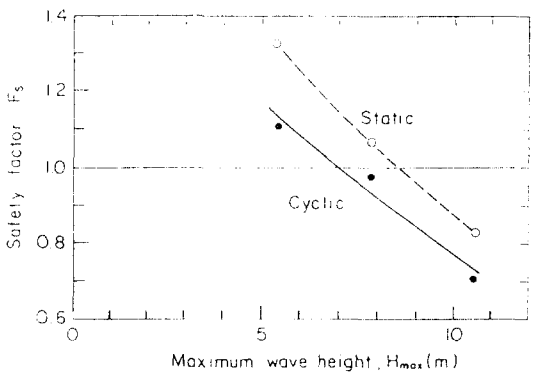

Fig. 12 Safety factor

6. CONCLUSIONS

The mechanism of the wave-driven liquefaction is discussed in the context of the excess pore pressure. There are two types of wave-driven liquefaction which are different in the mechanism of the excess pore pressure build-up; one is the liquefaction due to oscillatory excess pore pressures and the other is the liquefaction caused by residual excess pore pressures.

The procedures for assessing the excess pore pressures and liquefaction potential are presented and verified by model experiments and field data. The applicability of the proposed procedures is confirmed by case histories of damaged coastal structures. The procedures can be used to estimate the liquefaction potential in the permeable seabed.

The liquefaction potential or the excess pore pressure should properly be assessed for the design of coastal structure foundations and the estimation of seabed stability.

REFERENCES

1) Kang, H.Y. and Nielsen, P., "Watertable dynamics in coastal areas", *Proc. 25th Int. Conf. Coastal Engg.*, ASCE, Orlando, pp. 4601-4612, 1996

2) Lee, I.H., "A study on the wave-induced liquefaction of seabeds", *Ph.D. Thesis*, Natl. Fisher. Univ. Pusan, pp. 1-100, 1992

3) Zen, K. and Yamazaki, H., "Mechanism of wave-induced liquefaction and densification in seabeds", *Soils and Foundations*, 30(4), pp. 90-104, 1990

4) Ishihara, K. and Yamazaki, A., "Wave induced liquefaction in seabed deposits of sand", *Proc. IUTAM '83 Symp., Seabed Mechanics*, pp. 139-148, 1984

5) Lee, K.L. and Focht, J.A., "Liquefaction potential at Ekofish Tank in North Sea", *J. GE Div.*, ASCE, 101(1), pp. 1-18, 1975

6) Rahman, M.S., Seed H.B. and Booker, J.R., "Pore pressure development under offshore gravity structures", *J. GE Div.*, ASCE, 103 (12), pp. 1419-1436, 1978

7) Zen, K. and Yamazaki, H., "Oscillatory pore pressure and liquefaction in seabed induced by ocean waves", *Soils and Foundations*, 30(4), pp. 147-161, 1990

8) Zen, K. and Yamazaki, H., "Field observation and analysis of wave-induced lique-

faction in seabed", *Soils and Foundations*, 1991

9) Zen, K. and Umehara. Y., "Analysis on wave-induced pore pressure in sand layers under breakwater", *Proc. Intl. Symp. Ocean Space Utilization '85*, pp. 467-474, 1985

10) Zen, K., Umehara, Y. and Finn, W.D.L., "A case study of the wave-induced liquefaction of sand layers under the damaged breakwater", *Proc. 3rd Canadian Conf. on Marine Geotech.* Engg., Vol. 2, pp. 505-520, 1986